The Character and Formation of Elongated Depressions on the Upper Bulgarian Slope

XU Cuiling[1,2], GREINERT Jens[2*], HAECKEL Matthias[2], BIALAS Jörg[2], DIMITROV Lyubomir[3], ZHAO Guangtao[1]

1) College of Marine Geo-Sciences, Ocean University of China, Qingdao 266100, China
2) GEOMAR Helmholtz Centre for Ocean Research Kiel, Kiel 24148, Germany
3) Institute of Oceanology Bulgarian Academy of Science, Varna 9000, Bulgaria

Abstract Seafloor elongated depressions are indicators of gas seepage or slope instability. Here we report a sequence of slope-parallel elongated depressions that link to headwalls of sediment slides on upper slope. The depressions of about 250 m in width and several kilometers in length are areas of focused gas discharge indicated by bubble-release into the water column and methane enriched pore waters. Sparker seismic profiles running perpendicular and parallel to the coast, show gas migration pathways and trapped gas underneath these depressions with bright spots and seismic blanking. The data indicate that upward gas migration is the initial reason for fracturing sedimentary layers. In the top sediment where two young stages of landslides can be detected, the slope-parallel sediment weakening lengthens and deepens the surficial fractures, creating the elongated depressions in the seafloor supported by sediment erosion due to slope-parallel water currents.

Keywords: methane seepage, elongated depression, pockmark, landslide, Black Sea

1. Introduction

Seafloor elongated depressions, indicators for gas seepage or slope instability, have been reported from several continental margins, such as the West African margin, the Turkish Black Sea shelf, the mid-U.S. Atlantic coast, the Norwegian continental slope and the Santa Barbara Basin (Pilcher and Argent, 2007; Çifį et al., 2003; Driscoll et al., 2000; Newman et al., 2008; Mienert et al., 2010; Reiche et al., 2011; Laberg et al., 2013; Greene et al., 2006).

* GREINERT Jens
Email: jgreinert@geomar.de
Tel.: +49 431 600-2590

Two explanations are given for their formation mechanisms. One is linked to submarine gas release from "pockmarks" that are grouped together (Hovland et al., 2002; Bøe et al., 1998; Pilcher and Argent, 2007; Hill et al., 2004), the other is that they are opening tensional "cracks" as a result of slope instability. In the latter explanation they are regarded as the initial stage of a landslide (Laberg et al., 2013; Reiche et al., 2011; Martel, 2004; Greene et al., 2006).

On continental slopes, elongated depressions are often associated with both mass movement and gas seepage. So the initial reason for their occurrence is controversially discussed. Çifį et al. (2003), Hill et al. (2004) and Mienert et al. (2010) proposed that elongated depressions are created by gas seepage. In contrast, Driscoll et al. (2000), Martel (2004), Greene et al. (2006) and Reiche et al. (2011) suggested that in their study areas the elongated depressions are mainly a result of slope instability related to surrounding landslides or are influenced by older landslides further downslope. In our paper we discuss whether one of the two processes, gas seepage or sediment movement, is the main driver for the elongated depressions on the upper slope offshore southern Bulgaria, Black Sea.

Multibeam echosounder (MBES) data recorded during SPUX cruise with RV Akademik in 2012 show formerly reported 'pockmarks' (Dimitrov and Dontcheva, 1994) to be actually elongated depressions. Current and past gas seepage zones as well as different stages of landslides are identified by combining geological, geophysical and geochemical studies. We present the distribution and shape of the elongated depressions as well as their sub-surface structure to discuss the possible relationship between the elongated depressions and mass movement or gas seepage.

2 Geological setting

The Western Black Sea Basin (WBSB) is a back-arc basin that developed north of the Pontide Magmatic Arc as a consequence of the northward subduction of the Neo-Tethys oceanic plate. The study area is located on the submarine prolongation of the Balkan Orogen (Fig. 1; Georgiev, 2012). To the west the anticlinal structure of the West Achtopol Swell affects the Mid-Quaternary strata (Dimitrov and Dontcheva, 1994; Genov and Dimitrov, 2003).

The thickness of the overlying sedimentary strata on the basement increases seaward, from about 1.5 km at the upper slope to 3-3.5 km in the WBSB (Georgiev, 2012). The thickness of Quaternary sediments is more than 600 m at the slope base just seaward of the study area (Dimitrov and Dontcheva, 1994). Affected by global sea level change during the Quaternary,

the sedimentary environment of the Black Sea alternated between a saline sea and a fresh water lake (Ross, 1974). The superficial Holocene layers are silty clay enriched in organic matter (C_{org} 1-5 %) with a thickness of typically 2 m, but the underlying Upper Pleistocene sediments are lacustrine clayey mud with C_{org} concentrations of less than 1 %.

The pockmark zone reported by Dimitrov and Dontcheva (1994) is located at the shelf edge, while the southern part, resurveyed during the SPUX cruise, is located in the upper part of the continental slope. The pockmark zone is bounded by the Rezovo fault to the south. The northern bounding cannot be determined due to lack of data.

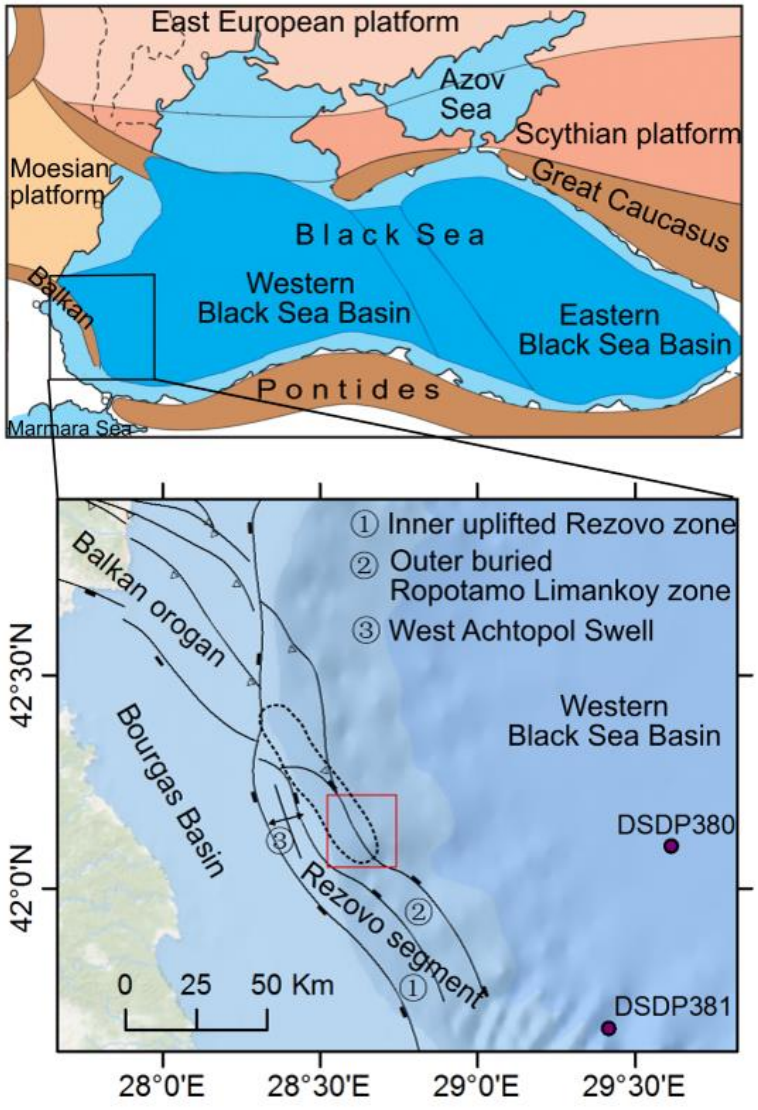

Fig. 1 Main structural features of the Bulgarian Black Sea zone (Georgiev, 2012). The study area is marked by red rectangle, the pockmark zone reported by Dimitrov and Dontcheva, (1994) are marked by dash line.

3. Materials and methods

More than 230 km^2 of seafloor were mapped with a Reson SeaBat 7111 MBES (100 kHz; 2° x 1.5° beam angle). The vessel velocity ranged from 3 to 5.2 kn during the surveys. Sound velocity information was acquired with a real time sound velocity probe near the transducers (Reson SVP-71). Sound velocity profiles were acquired during CTD casts. The Generic Mapping Tools (GMT 5.1; Wessel et al., 2013), Fledermaus (Version 7.4; from QPS) and ArcGIS (Version 10.1) software packages were used to visualize the data. Data processing was performed with PDS2000.

Twenty-eight seismic profiles were acquired using a sparker-streamer combination from RCMG (Gent University). The Applied Acoustics CSP600 power source (600 Joule) supplied energy to the sparker ELC820 (100 tips) at a 1.5 s shooting rate. The distance between shot points was about 2-3 m depending on ship speed. A single-channel streamer with 10 hydrophones was used for signal reception with the IXSEA Delph software (sampling interval of 100 µs or 125 µs). RadExPro and Seismic Unix were used as processing software, including smoothing the seafloor horizon by moving average with window size 9 (sea waves static), Stolt migration (using a constant sound velocity, ~ 1470 m/s) and band pass filtering (10 - 600 Hz). The Kingdom Suite Software (Version 2015) was used for interpretation and visualization.

4. Bathymetry of the study area

The study area is located on the shelf edge and the upper continental slope, with water depths of 110 to 600 m (Fig. 2). At the shelf break in about 140 m water depth the slope steepens from 0.5° to 1.2° at the outer shelf edge. The central part of the area shows a gentle terrain between 140m to 250 m water depths, where the slopes are steeper in the north (~1.8°) than in the south (1.2°). The eastern part of the area shows a more complex bathymetry. A multiphase landslide seafloor structure exists in the northeast, creating escarpments along its boundaries (Fig 2). In the southeast, the seafloor depth increased rapidly by about 400 m (Fig. 2), forming a valley as a result of the Rezovo fault described by Dimitrov and Dontcheva (1994). Between this valley and the landslide area, the seafloor appears as a saddle-shaped protrusion without clear slump features. Upslope of the landslide area and south of it, seventeen elongated depressions have developed almost parallel to the isobaths between 250 and 300 m water depth (Fig. 2 & 3).

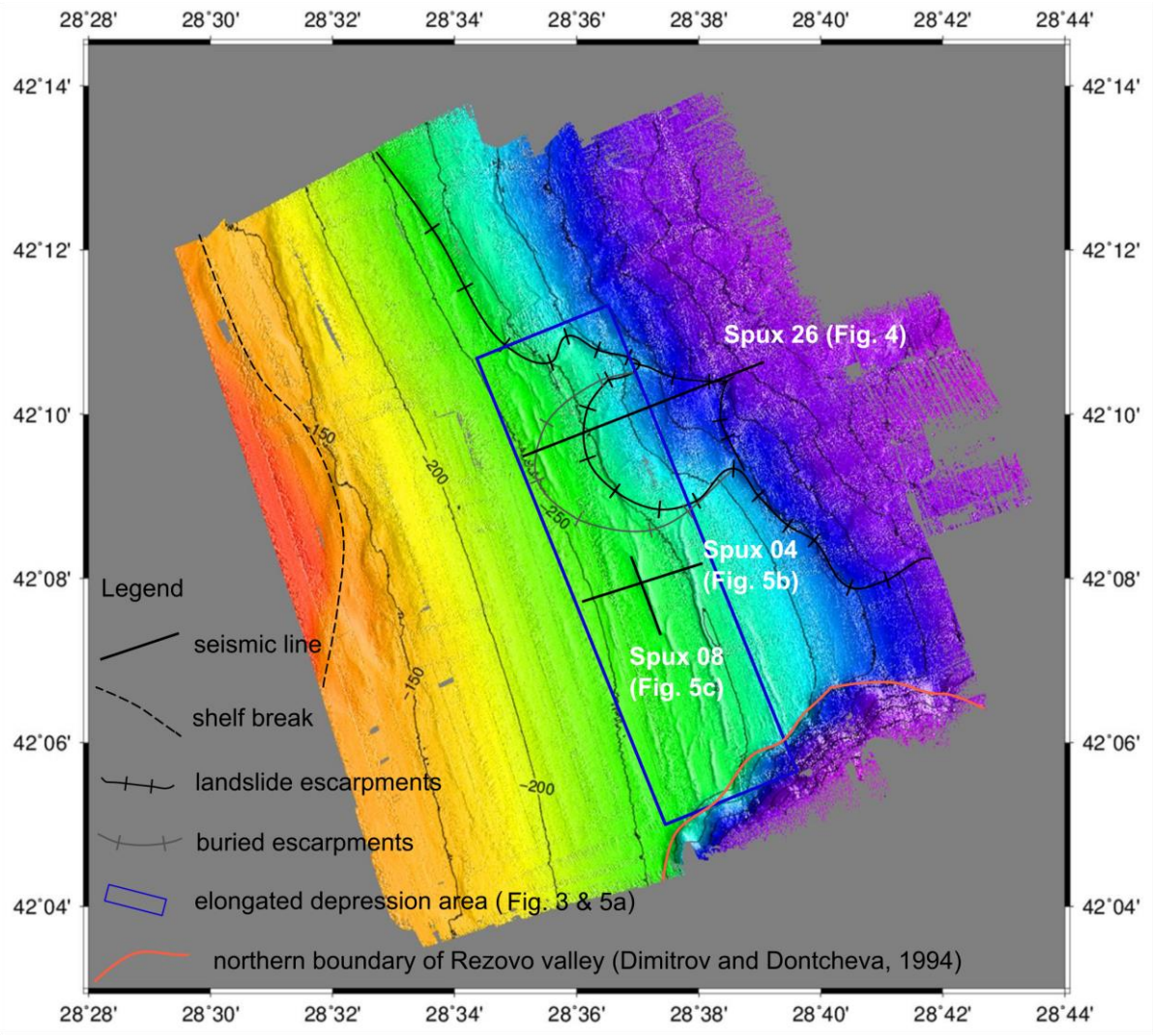

Fig. 2 Multibeam bathymetry map of the southern Bulgarian slope area, with indications for the shelf break, the northern boundary of the Rezovo valley, surface and buried slide escarpments as well as elongated depressions. Locations of seismic lines in Fig. 4 and 5 are indicated.

The lengths of the depressions range from 540 m to 3720 m and their width varies between 100 m and 300 m. The depressions are < 10 m deep with an average of about 5.5 ± 2 m. Most of the depressions are slightly curved, while some are bifurcated (depression #6, 7, 9 and 14; Fig. 3). The depressions are asymmetrical, and usually the upper (shallower) flanks have a steeper slope (2 - 6 º) than the lower flanks (2 - 4 º; Fig. 3b). The elongated depressions can be grouped into a southern (depression 1 - 10) and a northern group (depression 11 - 17), with landslide escarpments between them. Compared to the southern depressions, the northern group depressions are smaller. The average length of depressions in the south (1 – 10) is 2450 ± 1000 m with most of them being 1300 m to 3700 m long. The average length in the north

(11 – 17) is only 1280 ± 430 m. The average width and depth of the southern depressions (235 ± 50 m and 6.5 ± 2 m respectively) are larger than those found in the north (200 ± 50 m and 4 ± 0.8 m respectively).

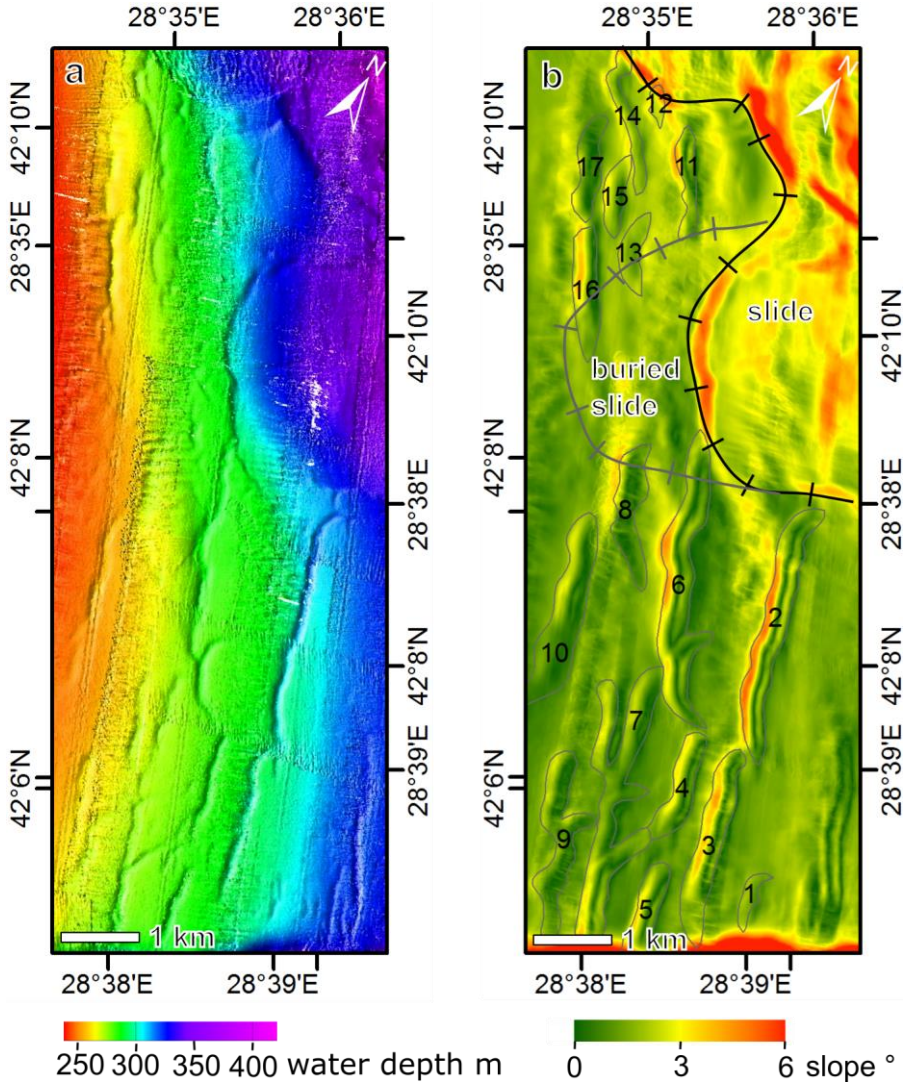

Fig. 3 Bathymetric map (a) and slope map (b) of the elongated depressions area (Fig. 2). Depressions are outlined by grey lines and numbered.

5. Seismic interpretation

The sparker seismic reflection profiles have imaged the sedimentary layers at the uppermost 150-300 ms of two-way travel time (TWT). In general, the reflectors are subparallel to the bathymetry dipping towards the basin in the east. Existing faults do not influence the Quaternary deposit structures significantly, except at the southeast part of the study site where the Rezovo fault shapes the Rezovo valley (Fig. 2, Dimitrov and Dontcheva, 1994). In the northeast, landslides are indicated by escarpments and chaotic reflections in the seismic

profiles (Fig. 4). Two slipping surfaces are clearly identified at ca. 90 -110 ms TWT and ca. 20 - 40 ms TWT below the seafloor. The deeper slipping surface also exists further downslope of all seafloor escarpments (indicated by both the grey and black lines in Fig. 2) and sedimentary layers above this slipping surface at 40 ms TWT are disturbed. The shallower slipping surface is located downslope of the seafloor escarpments (indicated by the black line in Fig. 2 and 4). Above this surface, either all sedimentary layers have been disturbed up to the seafloor, or the sedimentary layers have been disturbed as well except for the top ca. 10 ms TWT of the sediment.

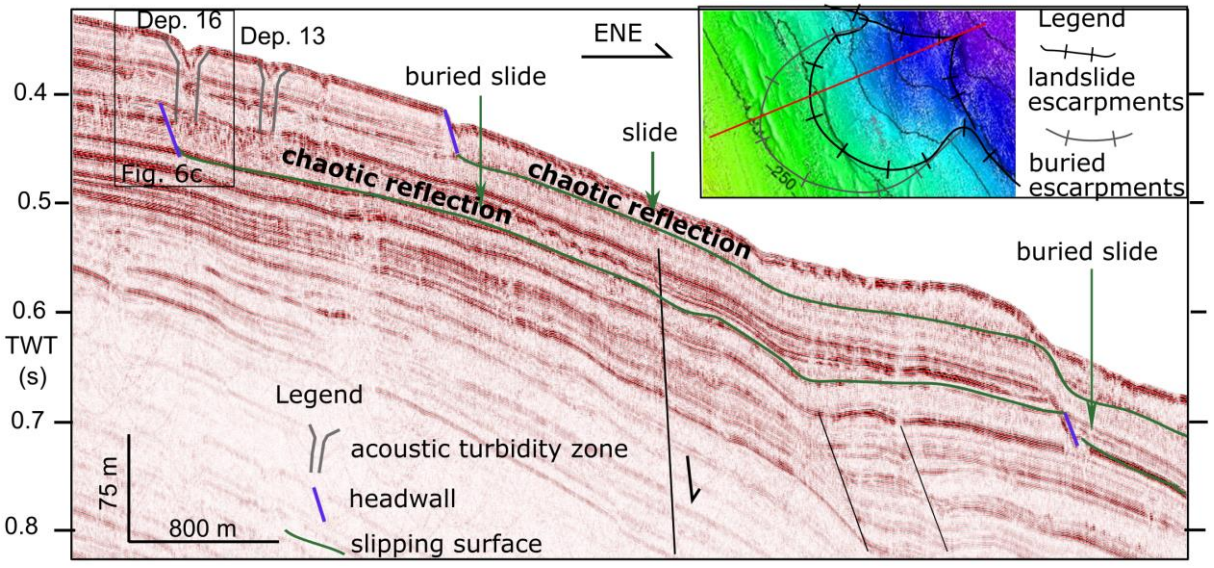

Fig. 4 The seismic profile Spux 26 (see Fig. 2 for location) shows slides and slide slipping surfaces as well as the subsurface structures of the elongated depressions that root at the buried slide.

Vertical acoustic turbidity zones and areas of high amplitudes with reverse polarity (gas pockets) which are typical for gas seepage areas can be seen below the depressions (Fig. 5b & c). The sub-bottom structure below the elongated depressions varies from one depression to the other. It also shows difference in lateral direction within the same depression. These differences are related to (1) the depths of the acoustic turbidity under the depressions, (2) the appearance of gas pockets, (3) the position of possible related landslides. Based on these differences, we classified the sub-bottom structures beneath the elongated depressions into three types, with a summary shown in Fig. 5a, and typical examples shown enlarged in Fig. 6.

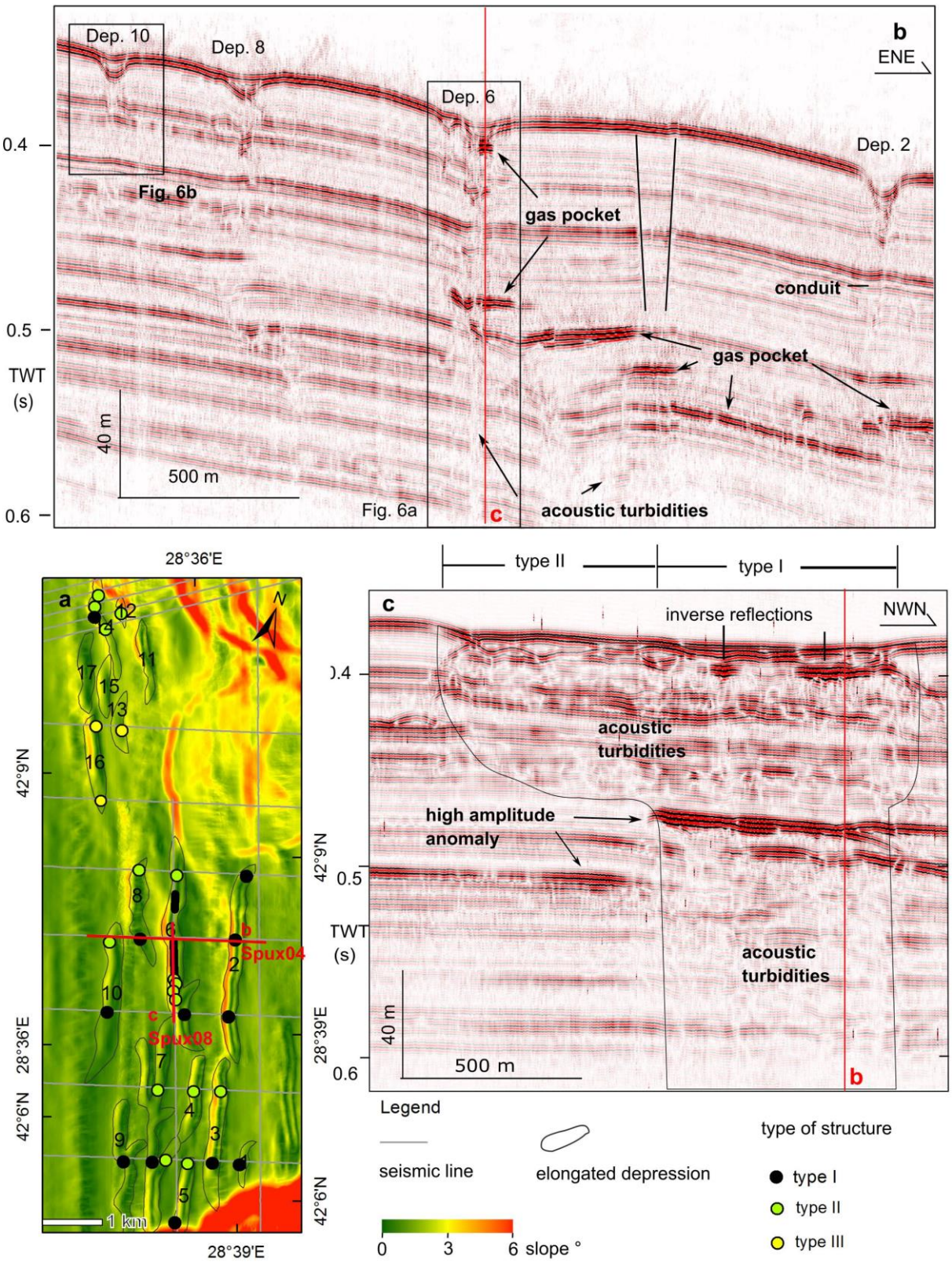

Fig. 5 (a) Overview of the three types of sub-surface structures under the depressions. Seismic line Spux 04 (b) runs perpendicular to depression 6 and Spux 08 (c) runs along its axis, showing the varying distribution of acoustic turbidity zones and gas pockets.

Type I—gas focusing conduits

For one set of depressions several seismic profiles show that the lower limit of the acoustic turbidity zone exceeds the recording depth of the sparker data (> 200 ms TWT below the seafloor, Fig. 6a). At least one profile of each depression in the southern group shows an acoustic turbidity zone deeper than 200 ms TWT below the seafloor, while only one profile shows a deep rooted acoustic turbidity zone underneath a depression in the north (Fig. 5a). Seismic profiles that lie perpendicular to the elongated depressions image a narrow acoustic turbidity zones (Fig. 5b), but show an acoustic turbidity zone at least 700 m long in profile Spux 08 that runs along depression 6 (Fig. 5c). This indicates that the acoustic turbidity zones are narrow cuboid volumes and not cylindrical isolated chimneys. These acoustic turbidity zones reach deeper than both slipping surfaces of landslides. Sedimentary layers on the two sides of the acoustic turbidity zones do not show a significant dislocation. In the area beneath the elongated depressions, gas pockets are common along the acoustic turbidity zones.

Type II—shallow rooted structure without gas pockets

In other seismic profiles the lower boundary of the acoustic turbidity zones could be imaged at 70 ms TWT below the seafloor (Fig. 6b). These acoustic turbidity zones cover the depth interval of the landslides. The sedimentary layers on both sides of the acoustic turbidity zones do not show a significant dislocation, and gas pockets are not found in these profiles.

Type III—structure rooted in the re-deposited landslides

The acoustic turbidity zones under depression 13 and 16 link to re-deposited sediments of buried landslides. The acoustic turbidity zones under depression 13 link to the chaotic reflections of a buried slide (Fig. 4), while turbidity areas under depression 16 just occur above the headwall of the slide (Fig. 4 & 6c). The acoustic turbidity zones root in the chaotic reflections of landslides, and do not penetrate the slipping surface.

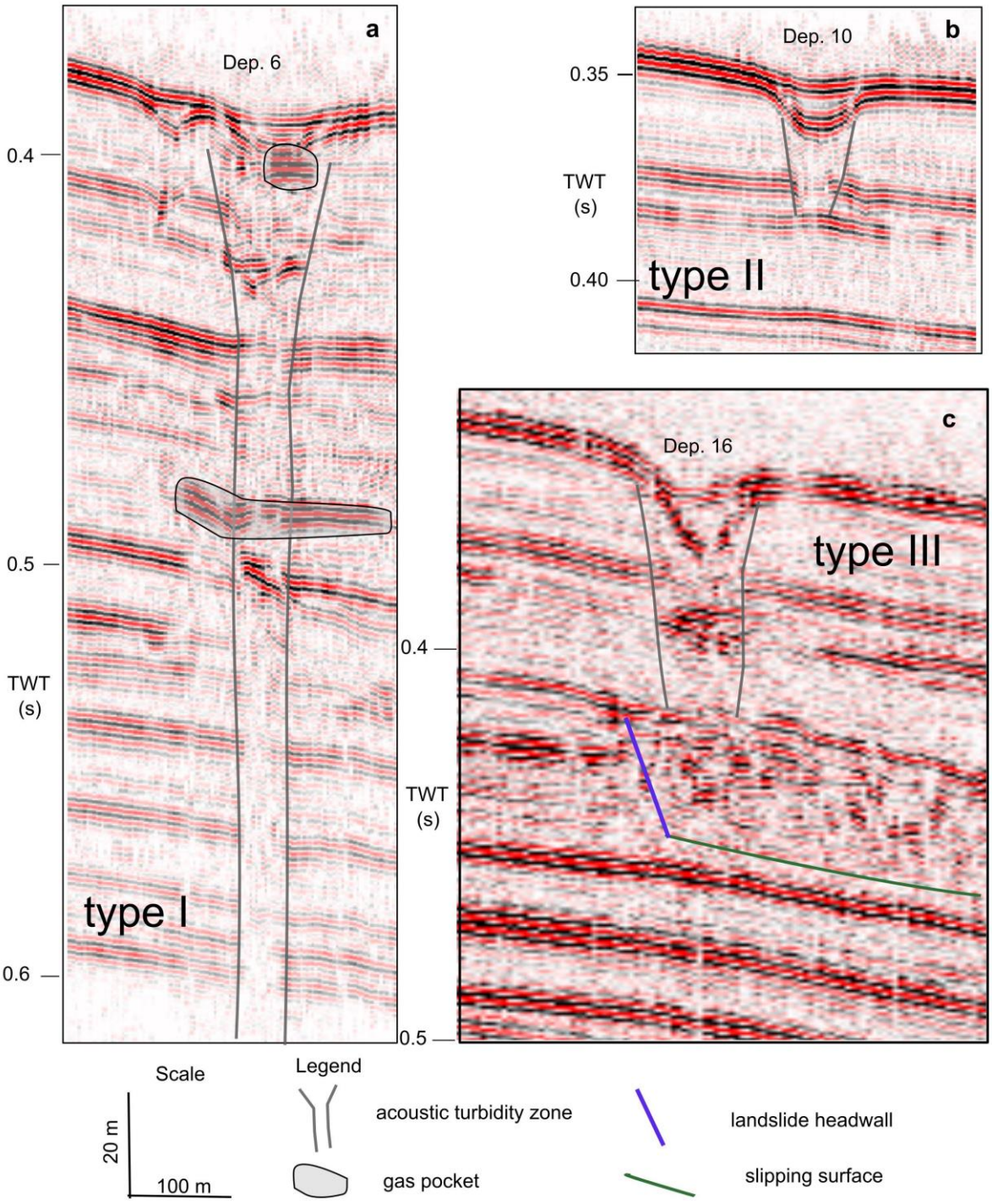

Fig. 6 The seismic profiles show three kinds of typical structures under the depressions. (a) type I -- the acoustic turbidity zone roots deeper than 200 ms TWT below the seafloor, and gas pockets are found. (b) type II -- the acoustic turbidity zone roots shallower than 30 ms TWT below the seafloor, and there are not gas pockets. (c) type III -- the acoustic turbidity zone roots in the buried landslides. See Fig. 5b for locations of profiles a and b, see Fig. 4 for location of profile c.

6. Discussion

The close proximity of landslides with elongated depressions and the presence of shallow gas pockets underneath these depressions imply that their location and formation results from a combined effect of slope instability and gas migration/seepage. Seafloor pockmarks have often been interpreted as indicators for (past) fluid/gas seepage and in some circumstances they have been found adjacent to and often upslope of landslides (Hovland et al., 2002). Typical examples are the Storegga Slide area at Nyegga, offshore mid-Norway (Reiche et al., 2011), the Baiyun Slide on the northern slope of the South China Sea (Li et al., 2014), the NG1 slide area in the north-east Atlantic (Riboulot et al., 2013), the Humboldt Slide offshore California (Yun et al., 1999) or the Albemarle Currituck slide area at the U.S. Atlantic margin (Hill et al., 2004; Newman et al., 2008). Çifį et al. (2003) proposed that elongated depressions (described by the authors as pockmarks) in the Turkish shelf of the Black Sea formed by the merging of circular pockmarks. However, most of the depressions in our survey area are kilometer scale, elongate features. Smaller circular pockmarks are not present in the research area (Fig. 2). Although a few depressions are slightly curved or bifurcate, the walls of the depressions are straight in general (Fig. 3). There is no clear evidence that individual circular pockmarks have been developed and thus the assumption that small circular pockmarks merged into elongated depressions seems unreasonable for the discussed research area.

Hill et al. (2004) and Newman et al. (2008) suggested that the elongated asymmetric depressions along the U.S. Atlantic margin (termed “gas blowouts”) formed primarily by gas expulsion due to tensional stress, and the related downslope creep of sediments is linked to gas release along the seafloor of the shelf edge. The depression shapes in our research area are highly elongated and asymmetric (Fig. 3), showing similar shapes as those along the U.S. Atlantic margin. Along the Bulgarian slope research area, gas pockets are found along the acoustic turbidity zones which root deeper than the recording depth of the sparker data (Fig. 5 & 6a), implying these turbidity zones (type I structure) are the main conduit for fluid migration. As the sedimentary layers on both sides of the acoustic turbidity zones do not show a significant dislocation, they are not formed by Quaternary faults (Fig. 5). These acoustic turbidity zones (> 200 ms TWT below the seafloor, Fig. 6a) reach deeper than the two detected slipping surfaces (Fig. 4), ruling out the possibility that they are formed by sedimentary instabilities that are related to sediment movement/landslides (Chapron et al., 2004; Baeten et al., 2013; Laberg et al., 2013). We suggest that these vertical acoustic

turbidity zones are primarily fractured by gas migration and then serve as conduits for following gas.

In contrast to many other more focused and round/oval 'gas chimneys', the gas conduits offshore Bulgaria have a more continuous wall-like shape that follows the elongated depressions at the seafloor surface (Fig. 5). The length of these gas-conduit walls can be laterally shorter than the depressions above. The wall-like shape of the conduits points to a tensional stress regime within the Quaternary sediments and they are present under each depression in the southern part of the working area (depression 1 to 10). In contrast, only one has been found under the northern group of depressions (depression 11-17). We interpret this as an artifact created by the limited coverage of seismic lines in the north (Fig. 5a). We thus suggest that the buoyancy induced gas migration through the sediment is responsible for the formation of the type I structure under the depressions, and that this controlled the location of the seafloor elongated depressions.

Considering only the process of gas migration as the reason for the depression formation is not comprehensive. This is because gas pockets are not found along type II and type III structures (Fig. 5a, 6b & c), which indicates that gas migration and trapping is/has been absent under some parts of the elongated depressions. Secondly, downslope sediment creeping, which is proposed to contribute shaping the feature of the "gas blowouts" along the U.S. Atlantic margin (Hill et al., 2004), is not found in our research area.

Tension fractures，which are regarded as the initial stages of slope failure (Driscoll et al., 2000; Reiche et al., 2011; Laberg et al., 2013; Greene et al., 2006; Baeten et al., 2013), are assumed to lengthen and shape the elongated depressions. Under some of them, acoustic turbidity zones occur in the same shallow depth down to 70 ms TWT below the seafloor (type II & III structures) and indications of landslides could be observed. This might implicate that the sedimentary slipping at this depth interval may have an influence on the formation of these acoustic turbidity zones, and thus the elongated shape of the seafloor depressions. Landslides accompanied by tension fractures have also been found in several other continental margins. For example, the extension of landslide headwalls as fractures, such as the cracks in the Santa Barbara Channel (Greene et al., 2006), has been confirmed by 3-D modelling to be shear fractures as described by Martel (2004). Cracks of the Norwegian continental slope (Laberg et al., 2013; Baeten et al., 2013) have been described at the upslope of landslide headwalls and were interpreted to be the result of tension fractures. Tension fractures are usually distributed en échelon as surficial expression (Laberg et al., 2013), while

the depressions in our study area are subparallel linear. The difference may be because of the influence of gas migrateion along the type I structure or the saddle-shaped seafloor (Fig. 2) on the stress distribution.

As a conceptual model, the following sequential stages of bubble migration, gas accumulation, sediment weakening and sediment sliding are considered as a likely process for the formation of the elongated depressions on the upper Bulgarian slope. With the accumulation of gas under impermeable sedimentary layers, especially in the area where the slope of the seafloor increases seaward (Fig. 7 stage 1), pore pressure increases initiating the breakthrough of gas bubbles at individual locations, a process similar to the formation of gas chimneys (Fig. 7 stage 2). The vertical weakening of the sediment due to buoyancy driven gas bubble migration that fractures the sediment define the upper border of subsequent mass movement, but also the location and orientation of the elongated depressions. Near the gas-weakened conduit(s), the potential of gravitational forces to cause fracturing is highest, and these areas may turn into a growing gas migration plane in parallel to the slope. This will develop over time in the observed acoustic turbid ‘conduit wall’ with gas pockets (Fig. 7 stage 3, e.g. the type I structure in Fig. 5c). In stage 4, tension fractures may either occur together with landslides during one mass movement event, or form when the support from downslope or underneath sedimentary layers weakens. The areas upslope of landslide, the lateral/slope parallel extension of landslide headwalls and sedimentary layers above buried landslides are the most likely positions for the development of tension fractures. Areas with already weakened sediment structures as the ‘conduit walls’ give priority to a further development of tensional fractures/cracks causing that acoustic turbidity zones in shallow sedimentary layers are lengthened and widened (e.g. the type II structure in Fig. 5c), creating asymmetric elongated depressions on the seafloor (Fig. 7 stage 4). In stage 5, the elongated depression and the underneath ‘conduit wall’ or tensional cracks might transform into headwalls of sliding sites, facilitating the upslope retrogression of mass movement. One of those headwalls forms a slope-parallel extension of the depression developed in the north of depression 6 (Fig. 3b).

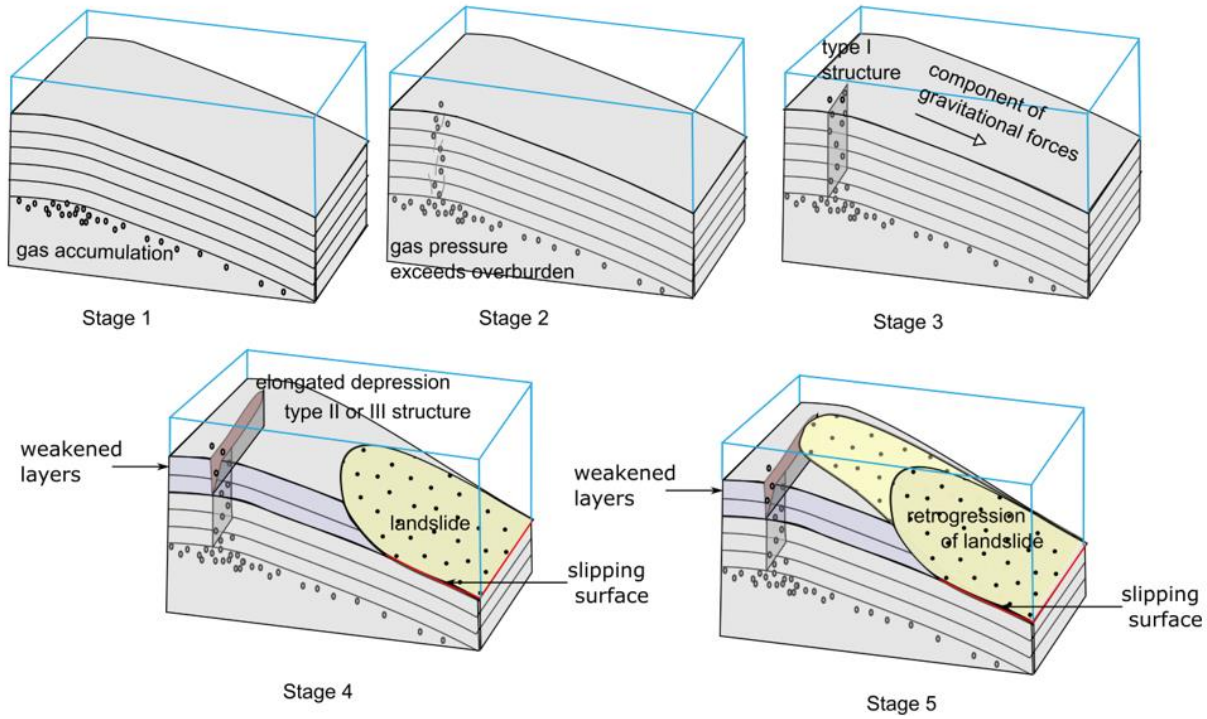

Fig. 7 Schematic outlining the formation process of elongated depressions. See text for explanation.

7 Conclusions

The series of asymmetric elongated depressions, imaged in seismic and multibeam-echo sounder data show a very close relation with gas migration and sediment sliding in the upper continental slope offshore southern Bulgaria. The lengths of the depressions range from 540 m to 3720 m, the widths vary between 100 m to 300 m, and their depths are < 10 m. Three types of vertical acoustic turbidity zones are found below the elongated depressions, including gas focus conduits that rooted deeper than the recording depth of the sparker data, shallow rooted structure without gas pockets, and structure rooted in the re-deposited landslides. The data imply that no faults existed prior to the onset of vertical gas migrations. However, once gas bubble migration started to weaken the sediments vertically and laterally, slope-parallel fracturing began to evolve. When the buoyancy of gas-charged fluids exceeds the overburden pressure, fluids and gas expelled through the overlying sediments, creating gas focusing conduits. At the depth interval of sediment sliding, conduits are lengthened and widened, developing into tensional fractures or cracks and so pre-defining/shaping the elongated depressions on the seafloor. The weakened surface sediments in the depressions are prone to be eroded by bottom currents which further help to deepen and widen these depressions until the observed stage.

Acknowledgements

We acknowledge the captains, the crew and technicians of the R/V Akademik for all support during the SPUX cruise in 2012. The cruise SPUX (AK211) has been funded by the European project EUROFLEETS (Seventh Framework Programme, grant agreement No. 228344) through transnational access to the research vessel "RV Akademik" operated by the Institute of Oceanology Bulgarian Academy of Science (Bulgaria). We thank Timo Zander, Peter Urban from GEOMAR for introductions to the Kingdom Suit software, and Linux programming, and Wei Li (from Kiel University) for seismic interpretation. We very much appreciated the comments of Prof. Marc De Batist from Gent University and two anonymous reviewers on an earlier version of this paper. We also thank Inken Preuss and Edna Hütten who were a great help in sorting out the English. This is publication 27 of the DeepSea Monitoring group at GEOMAR.

References

Baeten, N.J., Sverre, J., Forwick, M., Vorren, T.O., Vanneste, M., Fredrik, C., Kvalstad, T.J., Ivanov, M., 2013. Geomorphology Morphology and origin of smaller-scale mass movements on the continental slope off northern Norway. Geomorphology 187, 122–134. doi:10.1016/j.geomorph.2013.01.008

Bøe, R., Rise, L., Ottesen, D., 1998. Elongate depressions on the southern slope of the Norwegian Trench (Skagerrak): Morphology and evolution. Marine Geology 146, 191–203. doi:10.1016/S0025-3227(97)00133-3

Chapron, E., Van Rensbergen, P., De Batist, M., Beck, C., Henriet, J.P., 2004. Fluid-escape features as a precursor of a large sublacustrine sediment slide in Lake Le Bourget, NW Alps, France. Terra Nova 16, 305–311. doi:10.1111/j.1365-3121.2004.00566.x

Çifį, G., Dondurur, D., Ergün, M., 2003. Deep and shallow structures of large pockmarks in the Turkish shelf, Eastern Black Sea. Geo-Marine Letters 23, 311–322. doi:10.1007/s00367-003-0138-x

Dimitrov, L., Dontcheva, V., 1994. Seabed pockmarks in the southern Bulgarian Black Sea Zone. Bulletin of the Geological Society of Denmark 41, 24–33.

Driscoll, N.W., Weissel, J.K., Goff, J. a., 2000. Potential for large-scale submarine slope failure and tsunami generation along the U.S. mid-Atlantic coast. Geology 28, 407–410. doi:10.1130/0091-7613(2000)28<407: PFLSSF>2.0.CO;2

Genov, I., Dimitrov, O., 2003. Faults and Fault Activity Determined on the Basis of Seismic

343 Stratigraphy in the Region East from the West-Ahtopol Rise - Southern. Comptes
344 Rendus De Lacademie Bulgare Des Sciences 56, 71. doi:10.1007/s13398-014-0173-7.2
345 Georgiev, G., 2012. Geology and Hydrocarbon Systems in the Western Black Sea. Turkish
346 Journal of Earthences 21, 723–754. doi:10.3906/yer-1102-4
347 Greene, H.G., Murai, L.Y., Watts, P., Maher, N. a., Fisher, M. a., Paull, C.E., Eichhubl, P.,
348 2006. Submarine landslides in the Santa Barbara Channel as potential tsunami sources.
349 Natural Hazards & Earth System Sciences 6, 63–88. doi:10.5194/nhess-6-63-2006
350 Hill, J.C., Driscoll, N.W., Weissel, J.K., Goff, J. a., 2004. Large-scale elongated gas blowouts
351 along the U.S. Atlantic margin. Journal of Geophysical Research Atmospheres: Solid
352 Earth 109, B09101. doi:10.1029/2004JB002969
353 Hovland, M., Gardner, J. V., Judd, a. G., 2002. The significance of pockmarks to
354 understanding fluid flow processes and geohazards. Geofluids 2, 127–136.
355 doi:10.1046/j.1468-8123.2002.00028.x
356 Laberg, J.S., Baeten, N.J., Lågstad, P., Forwick, M., Vorren, T.O., 2013. Formation of a large
357 submarine crack during the final stage of retrogressive mass wasting on the continental
358 slope offshore northern Norway. Marine Geology 346, 73–78.
359 doi:10.1016/j.margeo.2013.08.008
360 Li, W., Wu, S., Wang, X., Zhao, F., Wang, D., Mi, L., Li, Q., 2014. Baiyun Slide and Its
361 Relation to Fluid Migration in the Northern Slope of Southern China Sea, in: Krastel, S.,
362 Behrmann, J.-H., Völker, D., Stipp, M., Berndt, C., Urgeles, R., Chaytor, J., Huhn, K.,
363 Strasser, M., Harbitz, C.B. (Eds.), 6th International Symposium on Submarine Mass
364 Movements and Their Consequences, Advances in Natural and Technological Hazards
365 Research. Springer International Publishing, Cham, pp. 105–115. doi:10.1007/978-3-
366 319-00972-8_10
367 Martel, S.J., 2004. Mechanics of landslide initiation as a shear fracture phenomenon. Marine
368 Geology 203, 319–339. doi:10.1016/S0025-3227(03)00313-X
369 Mienert, J., Vanneste, M., Haflidason, H., Bünz, S., 2010. Norwegian margin outer shelf
370 cracking: a consequence of climate-induced gas hydrate dissociation? International
371 Journal of Earth Sciences 99, 207–225. doi:10.1007/s00531-010-0536-z
372 Newman, K.R., Cormier, M.H., Weissel, J.K., Driscoll, N.W., Kastner, M., Solomon, E. a.,
373 Robertson, G., Hill, J.C., Singh, H., Camilli, R., Eustice, R., 2008. Active methane
374 venting observed at giant pockmarks along the U.S. mid-Atlantic shelf break. Earth &
375 Planetary Science Letters 267, 341–352. doi:10.1016/j.epsl.2007.11.053

376 Pilcher, R., Argent, J., 2007. Mega-pockmarks and linear pockmark trains on the West
377 African continental margin. Marine Geology 244, 15–32.
378 doi:10.1016/j.margeo.2007.05.002
379 Reiche, S., Hjelstuen, B.O., Haflidason, H., 2011. High-resolution seismic stratigraphy,
380 sedimentary processes and the origin of seabed cracks and pockmarks at Nyegga, mid-
381 Norwegian margin. Marine Geology 284, 28–39. doi:10.1016/j.margeo.2011.03.006
382 Riboulot, V., Cattaneo, a., Sultan, N., Garziglia, S., Ker, S., Imbert, P., Voisset, M., 2013.
383 Sea-level change and free gas occurrence influencing a submarine landslide and
384 pockmark formation and distribution in deepwater Nigeria. Earth & Planetary Science
385 Letters375, 78–91. doi:10.1016/j.epsl.2013.05.013
386 Ross, D.A., 1978. Black Sea Stratigraphy. Initial Report of the Deep Sea Drilling Project, vol.
387 42, 2. US Government Printing Office, Washington DC. 17–26.
388 Wessel, P., Smith, W.H.F., Scharroo, R., Luis, J., Wobbe, F., 2013. Generic Mapping Tools:
389 Improved Version Released. Eos Transactions American Geophysical Union 94, 409–
390 410. doi:10.1002/2013EO450001
391 Yun, J.W., Orange, D.L., Field, M.E., 1999. Subsurface gas offshore of northern California
392 and its link to submarine geomorphology. Marine Geology 154, 357–368.
393 doi:10.1016/S0025-3227(98)00123-6